Phosphorylation of the voltage-gated potassium channel Kv2.1 by AMP-activated protein kinase regulates membrane excitability

Phosphorylation of the voltage-gated potassium channel Kv2.1 by AMP-activated protein kinase regulates membrane excitability

Naoko Ikematsu[a,1], Mark L. Dallas[b,1], Fiona A. Ross[a], Ryan W. Lewis[c], J. Nicole Rafferty[c], Jonathan A. David[c], Rakesh Suman[b], Chris Peers[b,1], D. Grahame Hardie[a,1,2], and A. Mark Evans[c,1]

[a]College of Life Sciences, University of Dundee, Dundee, DD1 5EH, United Kingdom; [b]School of Medicine, University of Leeds, Leeds, LS2 9JT, United Kingdom; and [c]College of Medicine and Veterinary Medicine, University of Edinburgh, Edinburgh, EH8 9XD, United Kingdom

Edited by Richard L. Huganir, The Johns Hopkins University School of Medicine, Baltimore, MD, and approved September 27, 2011 (received for review April 21, 2011)

Firing of action potentials in excitable cells accelerates ATP turnover. The voltage-gated potassium channel Kv2.1 regulates action potential frequency in central neurons, whereas the ubiquitous cellular energy sensor AMP-activated protein kinase (AMPK) is activated by ATP depletion and protects cells by switching off energy-consuming processes. We show that treatment of HEK293 cells expressing Kv2.1 with the AMPK activator A-769662 caused hyperpolarizing shifts in the current–voltage relationship for channel activation and inactivation. We identified two sites (S440 and S537) directly phosphorylated on Kv2.1 by AMPK and, using phosphospecific antibodies and quantitative mass spectrometry, show that phosphorylation of both sites increased in A-769662–treated cells. Effects of A-769662 were abolished in cells expressing Kv2.1 with S440A but not with S537A substitutions, suggesting that phosphorylation of S440 was responsible for these effects. Identical shifts in voltage gating were observed after introducing into cells, via the patch pipette, recombinant AMPK rendered active but phosphatase-resistant by thiophosphorylation. Ionomycin caused changes in Kv2.1 gating very similar to those caused by A-769662 but acted via a different mechanism involving Kv2.1 dephosphorylation. In cultured rat hippocampal neurons, A-769662 caused hyperpolarizing shifts in voltage gating similar to those in HEK293 cells, effects that were abolished by intracellular dialysis with Kv2.1 antibodies. When active thiophosphorylated AMPK was introduced into cultured neurons via the patch pipette, a progressive, time-dependent decrease in the frequency of evoked action potentials was observed. Our results suggest that activation of AMPK in neurons during conditions of metabolic stress exerts a protective role by reducing neuronal excitability and thus conserving energy.

calcineurin | calcium signaling | energy homeostasis

AMP-activated protein kinase (AMPK) is a ubiquitously expressed sensor of cellular energy status (1). It is activated in response to increases in cellular AMP:ATP and ADP:ATP ratios by a mechanism involving allosteric activation and increased net phosphorylation at a conserved threonine (Thr172) mediated by the tumor-suppressor kinase, LKB1 (2). Thr172 phosphorylation and activation also can be triggered by increases in cytoplasmic Ca^{2+} via the calmodulin-dependent kinase calcium/calmodulin kinase kinase β (CaMKKβ) (1, 2). Although AMPK initially was thought to maintain cellular energy homeostasis primarily by regulating metabolism, emerging evidence suggests that it also modulates cell function by phosphorylating other targets, including ion channels. This function may be of particular significance in excitable cells such as central neurons. Remarkably, ATP turnover in rodent brain is comparable with that in human leg muscle during marathon running, and it has been estimated that action potentials account for 25–50% of this turnover, with synaptic transmission (triggered by action potentials) accounting for all but 15% of the remainder (3, 4). Voltage-gated K^+ (Kv) channels are crucial determinants of membrane excitability (5), and a major component of the delayed rectifier Kv current in cortical and hippocampal pyramidal neurons, especially in the somatodendritic region where they regulate firing of axonal action potentials, is provided by Kv2.1 (6). Changes in the level of phosphorylation within the cytoplasmic C-terminal tail of Kv2.1 have been proposed to underpin changes in its gating properties and thereby neuronal activity, especially during periods of metabolic stress such as hypoxia or ischemia (7, 8). We therefore investigated the possibility that AMPK might modulate neuronal excitability by direct phosphorylation and regulation of Kv2.1.

Results

AMPK Activation Causes Shifts in Voltage Dependence of Kv2.1 Gating. HEK293 cells stably expressing rat Kv2.1 (8) were treated with the AMPK activator A-769662 (9, 10), which caused maximal phosphorylation of acetyl-CoA carboxylase (ACC), a marker for AMPK activation, at 200 μM within 10 min (Fig. S1). Under these conditions A-769662 caused pronounced hyperpolarizing shifts in the current–voltage relationship for Kv2.1 activation and inactivation (Fig. 1*A*), with half-maximal steady-state activation ($G_{0.5}$) shifting from +15 ± 1.7 to −15 ± 1.9 mV (mean ± SEM), and half-maximal steady-state inactivation ($Vi_{0.5}$) shifting from −30 ± 0.9 to −52 ± 0.7 mV. These effects were abolished by preincubation with compound C. Although it is not a fully selective inhibitor of AMPK (11), reversal of the effects by compound C supports the view that A-769662 modifies Kv2.1 function by activating AMPK. It also was notable that the shifts in steady-state activation and inactivation were accompanied by increases in the rates of activation and inactivation (Fig. S2). These initial observations supported our hypothesis that AMPK reduces neuronal excitability by modulating Kv2.1 function.

AMPK Phosphorylates Kv2.1 at S440 and S537. To examine whether AMPK directly phosphorylates Kv2.1, we immunoprecipitated Kv2.1 from the HEK293 cells, treated with recombinant protein phosphatase (PP1γ) and then incubated with or without purified AMPK and [γ-^{32}P]ATP. We observed AMPK-dependent phos-

Author contributions: N.I., M.L.D., R.W.L., C.P., D.G.H., and A.M.E. designed research; N.I., M.L.D., R.W.L., J.A.D., and R.S. performed research; F.A.R. and J.N.R. contributed new reagents/analytic tools; N.I., M.L.D., C.P., D.G.H., and A.M.E. analyzed data; and N.I., M.L.D., C.P., D.G.H., and A.M.E. wrote the paper.

The authors declare no conflict of interest.

This article is a PNAS Direct Submission.

Freely available online through the PNAS open access option.

[1]N.I., M.L.D., C.P., D.G.H., and A.M.E. contributed equally to this work.

[2]To whom correspondence should be addressed. E-mail: d.g.hardie@dundee.ac.uk.

This article contains supporting information online at www.pnas.org/lookup/suppl/doi:10.1073/pnas.1106201108/-/DCSupplemental.

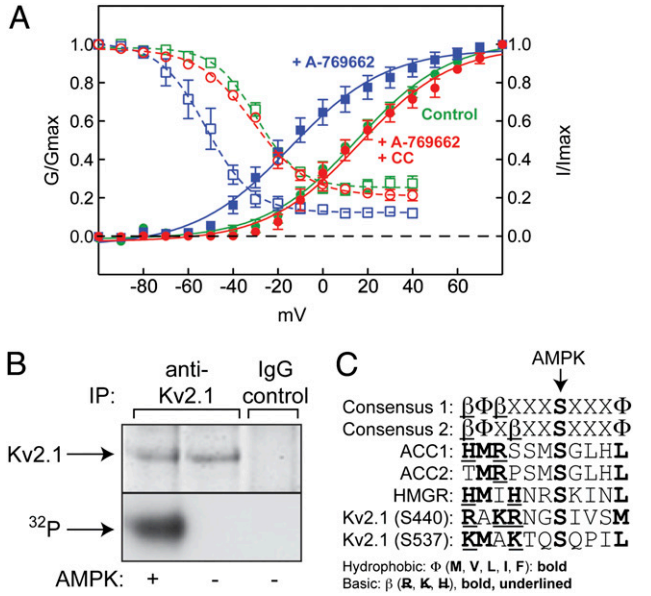

Fig. 1. Effects of A-769662 on Kv2.1 function in HEK293 cells and phosphorylation of Kv2.1 by AMPK in cell-free assays. (*A*) HEK293 cells stably expressing rat Kv2.1 (8) were incubated with A-769662 (100 μM) ± compound C (40 μM) for 20 min. Activation is indicated by filled symbols and continuous lines; inactivation is indicated by open symbols and dashed lines. Data points are mean ± SEM (n = 5–15). Curves were obtained by fitting to the sigmoidal Boltzmann equation. (*B*) Phosphorylation of Kv2.1 by AMPK in cell-free assays. Proteins were immunoprecipitated from HEK293 cells stably expressing rat Kv2.1 using anti-Kv2.1 or control Ig (IgG), incubated with [γ-^{32}P]ATP ± purified AMPK, and SDS gels were analyzed by protein staining (*Upper*) or autoradiography (*Lower*). (*C*) Alignment of the recognition motif for AMPK with sequences around sites on ACC1, ACC2, HMG-CoA reductase (HMGR), and Kv2.1. Basic and hydrophobic residues involved in recognition by AMPK are marked by bold type and/or underlining.

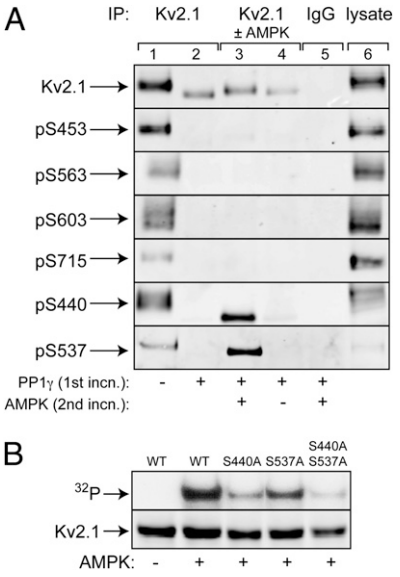

Fig. 2. Evidence that S440 and S537 are the major AMPK sites on Kv2.1. (*A*) Kv2.1 in immunoprecipitates made with anti-Kv2.1 (lanes 1–4) or control IgG (lane 5) or in a cell lysate (lane 6) was probed using anti-Kv2.1 or Kv2.1 phosphospecific antibodies. In lane 2, the immunoprecipitates were treated in a first incubation with phosphatase (PP1γ), and in lanes 3 and 4 this incubation was followed by a second incubation with ATP with or without AMPK. (*B*) Kv2.1 immunoprecipitated from cells expressing WT or S440A/S537A single or double mutants. Precipitates were treated with phosphatase PP1γ and then with [γ-^{32}P]ATP with or without AMPK.

phorylation of a polypeptide migrating with the expected mass of 95 kDa recovered using anti-Kv2.1 but not control Ig (Fig. 1*B*). The estimated stoichiometry of phosphorylation was 1.8 moles per mole of Kv2.1, indicating more than one site of phosphorylation. To identify sites, we digested with trypsin and carried out liquid chromatography-tandem MS (LC-MS:MS). We identified six unique phosphorylated residues (S440/S443/S453/S480/S645/S651) and eight phosphopeptides for which the exact site could not be identified because of multiple S/T residues. All lie within the C-terminal cytoplasmic domain (Fig. S3). Although multiple Kv2.1 phosphorylation sites have been identified previously [15, including S453, S480, and S651, in an analysis of rat Kv2.1 (8) and 11, including S440, S480, and S651, in an analysis of the mouse brain phosphoproteome (12)], the large number of sites found was surprising, given that we had pretreated with PP1γ before incubation with AMPK. However, this mass spectrometric methodology is not quantitative and also cannot distinguish between phosphate groups incompletely removed by PP1γ and those introduced by AMPK. Of the sites identified, only S440 and S537 are good fits to the established AMPK recognition motif (Fig. 1*C*). Both have basic residues at P−6 and P−4 and/or P−3, plus hydrophobic residues at P−5 and P+4, key determinants for AMPK recognition (13, 14) (although for S440 the hydrophobic residue at P−5 is alanine, whereas a bulkier residue is preferred).

We obtained phosphospecific antibodies against S453 and three other sites previously identified (S563/S603/S715) (8) and made phosphospecific antibodies against S440 and S537. Kv2.1 immunoprecipitated from untreated cells yielded signals with all six antibodies (Fig. 2*A*). As expected, all these signals were eliminated by PP1γ treatment, which also caused a marked increase in electrophoretic mobility of Kv2.1, consistent with dephosphorylation, as observed previously (7). After subsequent phosphorylation by AMPK, a small decrease in electrophoretic mobility was detected, but only signals obtained using pS440 and pS537 antibodies were restored (Fig. 2*A*). This result confirms that S440 and S537, but not S453, S563, S603, or S715, are phosphorylated by AMPK in cell-free assays. That S440 and S537 represent the major AMPK sites was confirmed when we made isogenic HEK293 cells stably expressing WT, S440A, S537A, or S440A/S537A substitutions of rat Kv2.1. The proteins were immunoprecipitated, treated with PP1γ, and incubated with or without AMPK and [γ-^{32}P]ATP, as before. As expected, single S440A or S537A substitutions reduced ^{32}P-labeling of Kv2.1 by AMPK, and a double substitution reduced it even further (Fig. 2*B*).

Shifts in Voltage Gating Caused by AMPK Require S440 Phosphorylation. In cells expressing WT Kv2.1, A-769662 caused phosphorylation (Thr172) and activation of AMPK (shown by phosphorylation of ACC) that was maximal at 100–200 μM and 10–20 min. It also increased phosphorylation of Kv2.1 at S440 and S537 (Fig. 3 *A* and *B*) but not at S453, S563, S603, or S715 (Fig. S4). Although the effects on S440/S537 phosphorylation were modest, the signals obtained using either antibody were eliminated in cells expressing the double substitution, confirming antibody specificity (Fig. 3*C*). We next assessed the effect of A-769662 on Kv2.1 phosphorylation more quantitatively using stable isotope labeling in culture (SILAC) using ^{13}C/^{15}*N*-labeled lysine/arginine. We identified 17 phosphorylation sites (Table S1), all except four of which had been identified previously (Fig. S3) (8). However, only three showed heavy:light (H:L) ratios >1.2, indicating increased phosphorylation in response to A-769662. The sites with the highest ratios were S440 (1.3-fold) and S537 (1.4-fold). In a repeat analysis, the H:L ratios for pS440 and pS537 were similar (1.3- and 1.5-fold, respectively).

Next, we analyzed the effects of A-769662 on the gating properties of Kv2.1 in the isogenic cell lines expressing each of

NEUROSCIENCE

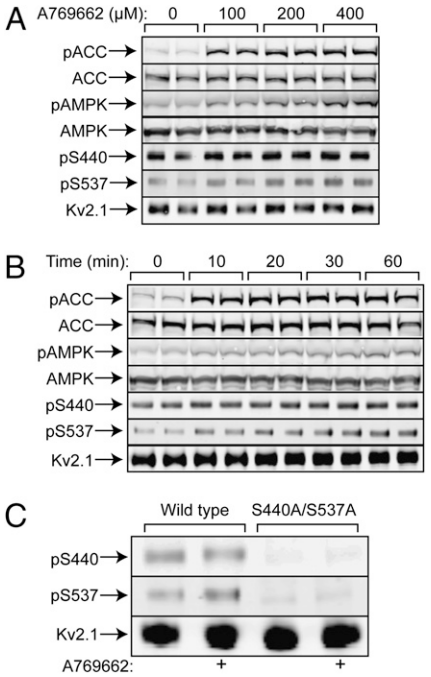

Fig. 3. Phosphorylation of ACC, AMPK, and Kv2.1 in response to A-769662 in isogenic HEK293 cells expressing Kv2.1 (duplicate cell incubations). (*A*) Effect of A-769662 concentration. (*B*) Time course. (*C*) Phosphorylation of S440/S537 in cells expressing either WT Kv2.1 or an S440A/S537A double mutant. Panels labeled pACC, pAMPK, pS440, and pS537 are Western blots obtained using appropriate phosphospecific antibodies.

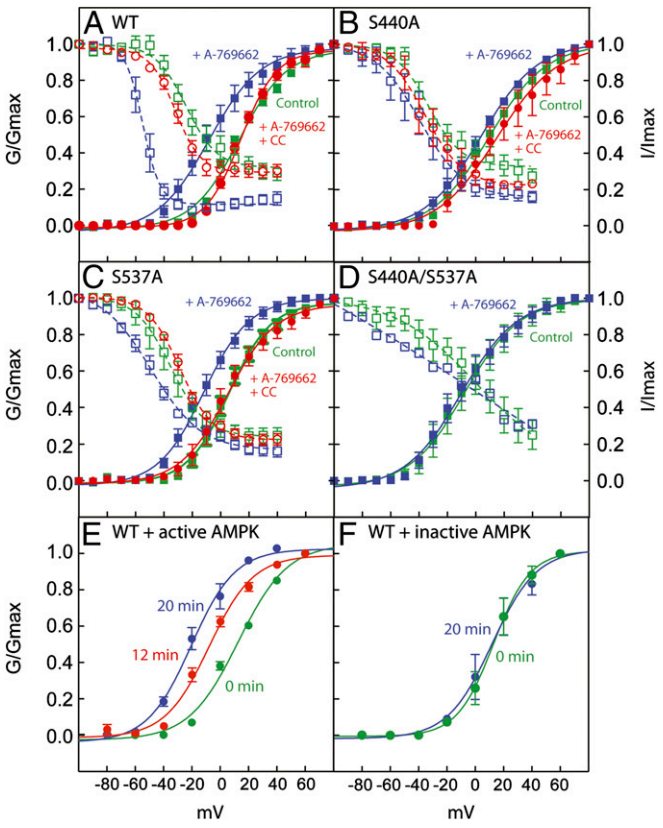

Fig. 4. Voltage–conductance plots showing effects of AMPK on voltage dependence of activation/inactivation in cells expressing WT or S440A/S537A single/double substitutions. (*A–D*) Effects of preincubation in the bath with A-769662 (100 μM, 20 min) ± compound C (40 μM). (*E* and *F*) Effect of intracellular dialysis with thiophosphorylated active or inactive AMPK introduced via the patch pipette. Individual data points are mean ± SEM (n = 7–10); results were fitted to the sigmoidal Boltzmann equation, and the curves were generated using the parameters shown in Table S2.

the Kv2.1 variants (Fig. 4 and Table S2). In WT cells a marked hyperpolarizing shift in steady-state activation, blocked by compound C, was observed (Fig. 4*A*) as seen previously with the independently generated WT cell line (Fig. 1*A*). This shift was reduced greatly with the S440A substitution (Fig. 4*B*); a small residual shift might appear to remain but was not statistically significant. For this mutant, effects on channel inactivation mirrored effects on activation; the large shift in $Vi_{0.5}$ (31 mV) in response to A-769662 in the WT cells was lost. The S537A substitution caused a small hyperpolarizing shift in activation (relative to WT) in untreated cells [as observed previously (8)], but a further shift of 18 mV in response to A-769662 (blocked by compound C) was still evident. With the double mutant the hyperpolarizing shift produced by A-769662 was abolished, but the mutations alone had a large effect, so that the double mutant had gating properties in untreated cells similar to those in WT after A-769662 treatment.

We also analyzed the effect of AMPK on channel function by applying, by intracellular dialysis via the patch pipette, bacterially expressed human AMPK (α2β2γ1 complex) that had been activated by thiophosphorylation at Thr172 with CaMKKβ [thiophosphorylated AMPK is completely resistant to phosphatases (15)] or an identically treated inactive mutant. In general, the results were very similar to those obtained when A-769662 was applied via the extracellular medium. The active AMPK (but not the inactive control) caused a progressive time-dependent hyperpolarizing shift in $G_{0.5}$ that was half-maximal at 12 min and maximal (33 mV) by 20 min (Fig. 4 *E* and *F* and Table S3).

Ionomycin Causes AMPK Activation and Shifts in Voltage Gating That Do Not Involve S440 Phosphorylation. In HEK293 cells expressing Kv2.1, the Ca^{2+} ionophore ionomycin induces a hyperpolarizing shift in voltage gating very similar to that caused by A-769662 in this study. However, this shift was proposed to be caused by dephosphorylation rather than by increased phosphorylation (8). Because increases in Ca^{2+} also can activate AMPK by the CaMKK pathway (1), we examined the effects of ionomycin on the phosphorylation of Kv2.1. Ionomycin caused activation of AMPK as assessed by increased phosphorylation of Thr172 on AMPK and its downstream target ACC. Interestingly, this activation was not associated with significant changes in phosphorylation of S440 or S537 on Kv2.1 (Fig. S5*A*). There was, however, a large dephosphorylation of S603, confirming previous results (8). We also analyzed ionomycin-induced changes in Kv2.1 phosphorylation by SILAC. This analysis revealed that seven sites were dephosphorylated (H:L < 0.8; Table S4), three of which (S11, S563, and S603) had been observed previously (8). However, phosphorylation of S440 and S537 was unchanged (H:L ~ 1.00). We also tested the effects of ionomycin on voltage gating in cells stably expressing Kv2.1, either WT cells or cells with S440A or S440D substitutions (Fig. S5 and Table S5). The cells with the S440D substitution, but not those with the S440A substitution, exhibited a hyperpolarizing shift of 16 mV relative to the WT cells, consistent with this substitution partially mimicking phosphorylation at S440. Ionomycin caused substantial shifts in gating in WT cells (20 mV) and in cells with the S440A substitution (21 mV) but not in cells with the S440D substitution.

AMPK Reduces Action Potential Frequency in Hippocampal Neurons. To examine the relevance of our findings in a more physiological setting, we examined the effect of A-769662 on K^+ currents in

cultured rat hippocampal neurons, measured after a prepulse to inactivate transient K^+ currents, thus isolating the delayed rectifier component. A-769662 caused a hyperpolarizing shift in gating of 14 mV (Fig. 5*A* and Table S6), similar to results in HEK293 cells expressing Kv2.1. After intracellular dialysis with Kv2.1 antibody through the pipette, there was a reduction in total current density (45 ± 7%, $P < 0.01$, $n = 5$), and the remaining current yielded a $G_{0.5}$ that was shifted in the hyperpolarizing direction by 9 mV compared with that before dialysis. However, there was no further shift in response to A-769662 (Fig. 5*B*), showing that the effect of A-769662 in untreated cells was caused entirely by modulation of Kv2.1.

It has been proposed that hyperpolarizing shifts in Kv2.1 voltage gating would reduce the frequency of repetitive action potential firing from a given excitatory input (6). To determine whether AMPK-dependent regulation of Kv2.1 might cause such an effect, we introduced the active thiophosphorylated α2β2γ1 complex or inactive control into the cultured hippocampal neurons via a patch pipette in whole-cell configuration in the current-clamp mode. Fig. 5 *C* and *E* show records of action potentials induced by current pulses in the same cell before and after intracellular dialysis (10 min); Fig. 5 *D* and *F* show results with the inactive control. As predicted, active but not inactive AMPK dramatically reduced the firing frequency. Fig. 5*G* shows plots of action potential frequency against time for several cells. After a lag of 2–4 min, the frequency was reduced progressively by intracellular dialysis of the active but not the inactive AMPK complex. There also was a small but significant hyperpolarization of the resting membrane potential (11.6 ± 3.6%; $P < 0.02$) and a small decrease in after-hyperpolarization amplitude (17.3 ± 6.6%; $P < 0.05$), but there were no significant changes in the duration, threshold, or amplitude of action potentials.

Discussion

Our results provide strong evidence that Kv2.1 is a direct target for AMPK at S440 and S537 and that phosphorylation of S440 and S537 by AMPK is associated with hyperpolarizing shifts in the voltage dependence of steady-state activation and inactivation of the channel. The S440A substitution abolished the effects of AMPK activation on voltage gating, identifying this site as being of primary importance for this effect. We suspect that phosphorylation of S537 has other functions. One puzzling feature is that although the shifts in voltage gating were quite large, the changes in phosphorylation of S440 were relatively small (~30%). Because Kv2.1 forms a homotetramer, one explanation is that there is a high basal phosphorylation of S440, but all four subunits must be phosphorylated to elicit an effect. A precedent is provided by the regulation of the BK_{Ca} ($K_{Ca}1.1$) channel by PKA, where phosphorylation of all four subunits of the homotetramer at S899 is required for channel activation (16).

Another surprising feature of our results was that phosphorylation of S440 by AMPK caused effects on Kv2.1 voltage gating very similar to those caused by ionomycin, which previously was shown to act by promoting dephosphorylation of Kv2.1 at multiple sites (8). Fig. S5*A* shows that ionomycin caused AMPK activation [presumably via Ca^{2+}/CaMKKβ-dependent phosphorylation of Thr-172, as in other cell types (17–19)]. However, using either phosphospecific antibodies or SILAC, we found that ionomycin did not change phosphorylation of S440 or S537, although, using SILAC, we detected dephosphorylation of seven other sites, including S563 and S603, as reported previously (8). Moreover, a similar shift in voltage gating by ionomycin was observed not only with WT Kv2.1 but also with an S440A mutant. By contrast, the S440D mutant exhibited a significant hyperpolarizing shift relative to the WT and the S440A mutant, although ionomycin had little further effect. These results confirm that the same change in voltage gating can be achieved via parallel, complementary pathways involving increased phosphorylation at S440 by AMPK or decreased phosphorylation at other sites (e.g., S563/S603) by calcineurin. The results with the S440D mutant suggest that these effects might not be additive.

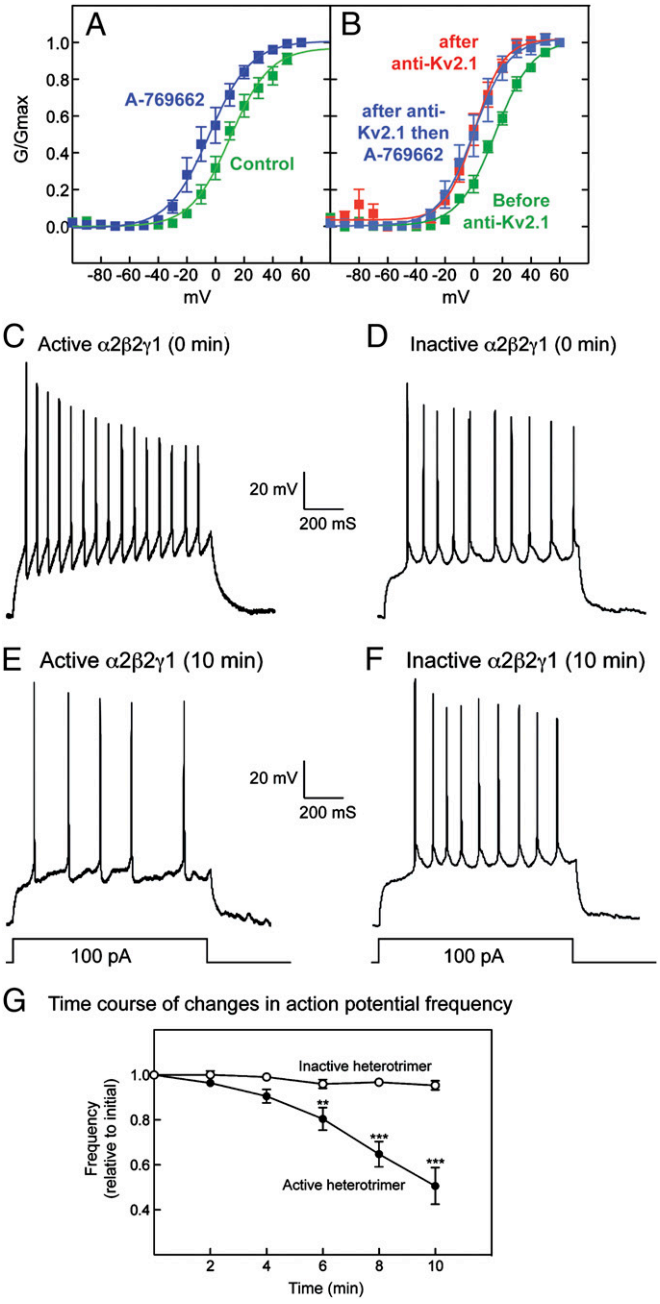

Fig. 5. Effect of AMPK on K^+ conductance and action potentials in cultured rat hippocampal neurons. (*A*) Voltage–conductance plot showing effects of A-769662 on the isolated K^+ delayed rectifier current in native hippocampal neurons. (*B*) Voltage–conductance plot for the K^+ delayed rectifier component in hippocampal neurons before/after intracellular dialysis of Kv2.1 antibody (anti-Kv2.1) and after subsequent application of A-769662. Individual data points are mean ± SEM ($n = 5$). Results were fitted to the sigmoidal Boltzmann equation, and the curves were generated using the parameters shown in Table S6. (*C–F*) Sample recordings from two cells at time 0 (*C* and *D*) and after intracellular dialysis for 10 min (*E* and *F*) of either active (*C* and *E*) or inactive (*D* and *F*) AMPK. (*G*) Action potential frequency (mean ± SEM of changes in individual cells over 10 min; $n = 7$; $^{**}P < 0.01$; $^{***}P < 0.001$, Dunnett's multiple comparison test). The mean initial frequencies of the cells injected with the active and inactive heterotrimers were 47 ± 7 and 41 ± 7 Hz, respectively.

Another question is why ionomycin did not cause S440 and S537 phosphorylation even though it activated AMPK. One explanation is that the pool of AMPK activated by A-769662 is in a subcellular location different from that activated by ionomycin. Interestingly, it has been shown (20) that AMPK activation using 2-deoxyglucose [which uses the classical AMP-dependent pathway (21)] occurs exclusively in the cytoplasm, whereas activation by Ca^{2+} ionophore also occurs in the nucleus.

Kv2.1 is expressed at high levels in the somatic and proximal dendritic regions of central neurons, where it regulates the initiation of axonal action potentials (6). Because of the slow kinetics of Kv2.1 activation and inactivation, it has been argued that hyperpolarizing shifts in voltage dependence would lead to progressive Kv2.1 opening in response to repetitive action potentials and would reduce the firing frequency of axonal action potentials (6). Indeed, glutamate suppresses the frequency of action potentials in cultured rat hippocampal neurons in a manner sensitive to the Kv2.1 inhibitor, hanatoxin (22). Our results show that endogenous Kv2.1 in hippocampal neurons, in which Kv2.1 contributes about half of the delayed rectifier current, is modulated by AMPK in the same manner as in HEK293 cells. Moreover, the introduction of a homogeneous, phosphatase-resistant AMPK via the patch pipette showed that AMPK reduces the firing of action potentials as predicted.

Our findings can be viewed as another illustration of the function of AMPK in conserving energy, in this case serving to protect central neurons against metabolic stress. AMPK-dependent phosphorylation of Kv2.1 may provide, via a Ca^{2+}-independent pathway, a mechanism complementary to that of calcineurin-dependent dephosphorylation that enhances the protection of neurons during periods of cerebral ischemia (7, 8). It also has been shown recently that voltage gating of Kv2.1 is modulated by SUMOylation (23).

Our results show that AMPK facilitates activation of a K^+ channel and consequent inhibition of neuronal excitability via direct phosphorylation at defined sites. They demonstrate that almost identical effects on Kv2.1 gating can be obtained by increased phosphorylation at S440 or by decreased phosphorylation at other sites mediated by calcineurin. S563 and S603 are the sites likely responsible for the latter effect, because both we and Park, et al. (8) found these sites were dephosphorylated after ionomycin administration, and a double S563A/S603A substitution caused a shift in gating almost as large as that induced by ionomycin (8).

In contrast to the present results, AMPK has been reported to phosphorylate and inactivate other K^+ channels, including the Ca^{2+}-activated K^+ channels $K_{Ca}1.1$ and $K_{Ca}3.1$ and the pore-forming subunit of the K_{ATP} channel (Kir6.2) (24–27). Our results suggest that AMPK can increase or decrease cell excitability, determined by cell-specific expression of members of the K^+ channel superfamily. AMPK therefore offers great versatility in its capacity to regulate metabolic status at the cellular and whole body levels.

Materials and Methods

Sources of proteins, antibodies, and other materials and methods used for cell culture and immunoprecipitation of Kv2.1 from cell extracts are given in *SI Materials and Methods*.

Tetracycline-Inducible Stable HEK293 Cell Line Expressing Rat Kv2.1. HEK293 host cells containing a single flippase recognition target (FRT) site and also independently incorporated pcDNA6/TR (Invitrogen) were transfected with Polyfect (QIAGEN) using the plasmids pOG44 and pcDND5/FRT/TO/Kv2.1 at a ratio of 9:1. Fresh medium was added to the cells 24 h after transfection, and medium containing 200 μg/mL hygromycin B was added 48 h after transfection. The medium was replaced every 3 d until foci could be identified; then individual foci were selected and expanded. The expression of Kv2.1 was checked using immunofluorescence microscopy and Western blotting using mouse anti-Kv2.1 α subunit antibodies (clone K89/34, NeuroMab).

In Vitro Phosphorylation of Kv2.1 by AMPK. Washed immunoprecipitates of recombinant rat Kv2.1 from HEK293 cells were incubated with PP1γ for 20 min at 30 °C, followed by extensive washing with ice-cold lysis buffer and then Hepes buffer [50 mM Na Hepes (pH 7.4), 1 mM DTT). The precipitate was incubated with 5 mM $MgCl_2$, 200 mM [γ-^{32}P]ATP, 8 μM okadaic acid, with or without AMPK purified from rat liver (28) (5 U/mL in the presence of 200 μM AMP; Fig. 1*B*) or bacterially expressed AMPK (α2β2γ1, 10 U/mL, previously activated using CAMKKβ and ATP) (15) (Figs. 2–5) for 30 min at 30 °C. After being washed five times with ice-cold Hepes buffer, the proteins were boiled with lithium dodecyl sulfate sample buffer and subjected to Tris-acetate SDS gel electrophoresis (Invitrogen). Incorporation of ^{32}P was determined as described previously (25). For the experiment shown in Fig. 1*D*, immunoprecipitates were incubated with unlabeled ATP in place of [γ-^{32}P]ATP and were analyzed by Western blotting with anti-Kv2.1 or phosphospecific antibodies as indicated.

Identification of Phosphorylation Sites by LC-MS/MS. Lysate (2.8 mg) from HEK293 cells expressing Kv2.1 was immunoprecipitated with 100 μg of Kv2.1 antibody and then incubated with PP1γ followed by phosphorylation by AMPK as described above, except that [γ-^{32}P]ATP was replaced by unlabeled ATP. The gel was visualized by staining with Colloidal Blue (Invitrogen). The excised gel band was analyzed as described previously (29).

SILAC. HEK293 cells were grown for >1 wk in Arg0-, Lys0-, or Arg6/Lys8-labeling DMEM (Dundee Cell Products) containing charcoal-filtered FBS, 100 IU/mL penicillin, 100 μg/mL streptomycin, and 200 μg/mL hygromycin B. Tetracycline (100 ng/mL) was added 24 h before treatment. After treatment ± 200 μM A-769662 for 20 min, lysates were prepared as described above. The labeled and unlabeled lysates were combined 1:1 according to protein content. The pooled lysates was preincubated with protein G-Sepharose for 1 h at 4 °C followed by incubation with anti-Kv2.1 antibody and protein G-Sepharose overnight at 4 °C. The precipitates were subjected to Tris-acetate SDS gel electrophoresis and visualized by Colloidal Blue staining. The sample was analyzed as described above. Before application to the HPLC column, trypsin-digested peptides were purified using a TiO_2 column (30) to enrich phosphorylated peptides. The raw data were analyzed with MaxQuant software.

Primary Culture of Hippocampal Neurons. Hippocampi from 6- to 8-d-old Wistar rats were removed for mechanical and enzymatic dissociation. Tissue was incubated for 15 min at 37 °C in PBS containing 0.25 μg/mL trypsin (EC 4.4.21.4, from bovine pancreas; Sigma). Trypsin digestion was terminated by the addition of an equal volume of buffer containing 16 μg/mL soybean trypsin inhibitor (SBTI, type I-S; Sigma), 0.5 μg/mL DNaseI (EC 3.1.21.1 type II from bovine pancreas; 125 kU/mL; Sigma) and 1.5 mM $MgSO_4$. Following centrifugation at 1,400 × *g* for 5 min, cells were resuspended in minimal Earle's medium with 10% FCS, 19 mM KCl, 13 mM glucose, 50 IU/mL penicillin, and 50 μg/mL streptomycin. One hundred microliters of cell suspension was plated onto poly-L-lysine–coated coverslips (10-mm diameter) in a 24-well plate for electrophysiology. Medium was replaced after 24 h with medium containing 10% (vol/vol) horse serum in place of FCS and 80 μM fluorodeoxyuridine to prevent the proliferation of nonneuronal cells. After 48 h the medium was exchanged for one containing Neurobasal medium, supplemented with 2% B-27, 1% penicillin/streptomycin, 0.5 mM L-glutamine, and 25 μM L-glutamic acid. Cells were maintained in a humidified incubator at 37 °C, 95% air/5% CO_2 for 14 d, with medium replaced every 5–7 d. All experiments were performed with cells cultured for 5–14 d.

Electrophysiology. ***HEK293 cells.*** Fragments of coverslip with attached Kv2.1-expressing HEK293 cells were transferred to a recording chamber, perfused at 3–5 mL/min [10 mM Na Hepes (pH 7.2), 140 mM NaCl, 5 mM KCl, 2 mM $MgCl_2$, 2 mM $CaCl_2$, 10 mM glucose), and mounted on the stage of an Olympus CK40 inverted microscope. K^+ currents were recorded by whole-cell patch clamp and evoked by a series of depolarizing steps from −90 to +80 mV in 10-mV increments for 500 ms. Recordings were at 37 °C unless otherwise indicated. Patch pipettes had resistances of 4–6 MΩ. Series resistance was monitored and compensated (60–80%) after achieving the whole-cell configuration. If a significant (>20%) increase occurred during the recording, the experiment was terminated. The pipette solution consisted of 10 mM Na Hepes (pH 7.2), 140 mM KCl, 5 mM EGTA, 2 mM $MgCl_2$, 1 mM $CaCl_2$, and 10 mM, glucose. For some experiments a thiophosphorylated AMPK complex (α2β2γ1, 2 U/mL) (15) was added to the pipette solution. The control was identical except for a D157A mutation in α1 to render the kinase inactive and was added at the same concentration. Conductance values (G) were calculated from the equation G = I/(V − EK), where the Nernst equilibrium potential EK was calculated as −89 mV at 37 °C. Normalized con-

ductance/voltage profiles for the Kv2.1 channel were fitted to a single Boltzmann function with the form G = Gmax/(1 + exp[− (V − V1/2)/*k*]), where Gmax is the maximal conductance, V1/2 is the test potential at which Kv2.1 channels have a half-maximal conductance ($G_{0.5}$), and *k* represents the slope of the activation curve. Signals were sampled at 10 kHz and low-pass filtered at 2 kHz. Voltage-clamp and analysis protocols were performed using an Axopatch 200A amplifier/Digidata 1200 interface controlled by Clampex 9.0 software (Molecular Devices). Off-line analysis was performed using Clampfit 9.0 (Molecular Devices).

Hippocampal neurons. For voltage-clamp experiments, the protocol was similar to that used for the HEK293 cells except for the inclusion of a single 30-ms prepulse to −10 mV to inactivate transient K^+ currents; the neurons also were held at −70 mV. Signals were sampled at 10 kHz and low-pass filtered at 2 kHz. For some experiments, an anti-Kv2.1 antibody (Neuromab) was added to the intracellular solution to give a final concentration of 0.5 μg/mL Action potential recordings were made in whole-cell current-clamp mode at 37 °C. Signals were low-pass filtered at 1 kHz and sampled at 10 kHz. Action potentials were evoked by 1-s current pulses (50–200 pA) at 0 and 10 min. Additionally, action potentials were evoked every 2 min during the experiments with a 100-pA current pulse. Patch electrodes (3–5 MΩ) contained 11 mM K Hepes (pH 7.2), 117 mM KCl, 10 mM NaCl, 11 mM EGTA, 2 mM Na_2ATP, 2 mM $MgCl_2$, 1 mM $CaCl_2$, and 0.3 mM NaGTP. Perfusate contained 117 mM NaCl, 4.5 mM KCl, 2.5 mM $CaCl_2$, 1 mM $MgCl_2$, 23 mM $NaHCO_3$, and 11 mM glucose and was bubbled with mixed gas (95% air/5% CO_2; pH 7.4). In some experiments a thiophosphorylated AMPK complex ($\alpha2\beta2\gamma1$) or a D157A inactive control was added to the patch pipette at a concentration of 2 U/mL or the equivalent concentration for the inactive mutant (15). Action potential parameters were measured off-line from the first action potential generated in response to a 100-pA stimulus, using Clampfit 9.0 (Molecular Devices). Firing frequency was determined from the interspike interval between the first two action potentials.

ACKNOWLEDGMENTS. We are grateful to Ashleigh Evans, Greg Stewart, and Douglas Lamont (University of Dundee) for assistance with developing antibodies and mass spectrometry and James Trimmer for providing the Kv2.1-expressing cell line used in Fig. S1 and phosphospecific antibodies. This research was supported by Wellcome Trust Program Grants 081195 (to C.P., D.G.H., and A.M.E.) and 080982 (to D.G.H.).

1. Hardie DG (2007) AMP-activated/SNF1 protein kinases: Conserved guardians of cellular energy. *Nat Rev Mol Cell Biol* 8:774–785.
2. Hardie DG, Carling D, Gamblin SJ (2011) AMP-activated protein kinase: Also regulated by ADP? *Trends Biochem Sci* 36:470–477.
3. Attwell D, Laughlin SB (2001) An energy budget for signaling in the grey matter of the brain. *J Cereb Blood Flow Metab* 21:1133–1145.
4. Sengupta B, Stemmler M, Laughlin SB, Niven JE (2010) Action potential energy efficiency varies among neuron types in vertebrates and invertebrates. *PLOS Comput Biol* 6:e1000840.
5. Pongs O (1999) Voltage-gated potassium channels: From hyperexcitability to excitement. *FEBS Lett* 452:31–35.
6. Misonou H, Mohapatra DP, Trimmer JS (2005) Kv2.1: A voltage-gated K+ channel critical to dynamic control of neuronal excitability. *Neurotoxicology* 26:743–752.
7. Misonou H, Mohapatra DP, Menegola M, Trimmer JS (2005) Calcium- and metabolic state-dependent modulation of the voltage-dependent Kv2.1 channel regulates neuronal excitability in response to ischemia. *J Neurosci* 25:11184–11193.
8. Park KS, Mohapatra DP, Misonou H, Trimmer JS (2006) Graded regulation of the Kv2.1 potassium channel by variable phosphorylation. *Science* 313:976–979.
9. Cool B, et al. (2006) Identification and characterization of a small molecule AMPK activator that treats key components of type 2 diabetes and the metabolic syndrome. *Cell Metab* 3:403–416.
10. Göransson O, et al. (2007) Mechanism of action of A-769662, a valuable tool for activation of AMP-activated protein kinase. *J Biol Chem* 282:32549–32560.
11. Bain J, et al. (2007) The selectivity of protein kinase inhibitors: A further update. *Biochem J* 408:297–315.
12. Wiśniewski JR, Nagaraj N, Zougman A, Gnad F, Mann M (2010) Brain phosphoproteome obtained by a FASP-based method reveals plasma membrane protein topology. *J Proteome Res* 9:3280–3289.
13. Scott JW, Norman DG, Hawley SA, Kontogiannis L, Hardie DG (2002) Protein kinase substrate recognition studied using the recombinant catalytic domain of AMP-activated protein kinase and a model substrate. *J Mol Biol* 317:309–323.
14. Gwinn DM, et al. (2008) AMPK phosphorylation of raptor mediates a metabolic checkpoint. *Mol Cell* 30:214–226.
15. Ross FA, et al. (2011) Selective expression in carotid body type I cells of a single splice variant of the large conductance calcium- and voltage-activated potassium channel confers regulation by AMP-activated protein kinase. *J Biol Chem* 286:11929–11936.
16. Tian L, et al. (2004) Distinct stoichiometry of BKCa channel tetramer phosphorylation specifies channel activation and inhibition by cAMP-dependent protein kinase. *Proc Natl Acad Sci USA* 101:11897–11902.
17. Hawley SA, et al. (2005) Calmodulin-dependent protein kinase kinase-beta is an alternative upstream kinase for AMP-activated protein kinase. *Cell Metab* 2:9–19.
18. Hurley RL, et al. (2005) The Ca2+/calmodulin-dependent protein kinase kinases are AMP-activated protein kinase kinases. *J Biol Chem* 280:29060–29066.
19. Woods A, et al. (2005) Ca2+/calmodulin-dependent protein kinase kinase-beta acts upstream of AMP-activated protein kinase in mammalian cells. *Cell Metab* 2: 21–33.
20. Tsou P, Zheng B, Hsu CH, Sasaki AT, Cantley LC (2011) A fluorescent reporter of AMPK activity and cellular energy stress. *Cell Metab* 13:476–486.
21. Hawley SA, et al. (2010) Use of cells expressing gamma subunit variants to identify diverse mechanisms of AMPK activation. *Cell Metab* 11:554–565.
22. Mohapatra DP, et al. (2009) Regulation of intrinsic excitability in hippocampal neurons by activity-dependent modulation of the KV2.1 potassium channel. *Channels (Austin)* 3:46–56.
23. Plant LD, Dowdell EJ, Dementieva IS, Marks JD, Goldstein SA (2011) SUMO modification of cell surface Kv2.1 potassium channels regulates the activity of rat hippocampal neurons. *J Gen Physiol* 137:441–454.
24. Evans AM, et al. (2005) Does AMP-activated protein kinase couple inhibition of mitochondrial oxidative phosphorylation by hypoxia to calcium signaling in O_2-sensing cells? *J Biol Chem* 280:41504–41511.
25. Wyatt CN, et al. (2007) AMP-activated protein kinase mediates carotid body excitation by hypoxia. *J Biol Chem* 282:8092–8098.
26. Klein H, et al. (2009) Inhibition of the KCa3.1 channels by AMP-activated protein kinase in human airway epithelial cells. *Am J Physiol Cell Physiol* 296:C285–C295.
27. Chang TJ, et al. (2009) Serine-385 phosphorylation of inwardly rectifying K+ channel subunit (Kir6.2) by AMP-dependent protein kinase plays a key role in rosiglitazone-induced closure of the K(ATP) channel and insulin secretion in rats. *Diabetologia* 52: 1112–1121.
28. Hawley SA, et al. (1996) Characterization of the AMP-activated protein kinase kinase from rat liver and identification of threonine 172 as the major site at which it phosphorylates AMP-activated protein kinase. *J Biol Chem* 271:27879–27887.
29. Sullivan S, Thomson CE, Lamont DJ, Jones MA, Christie JM (2008) In vivo phosphorylation site mapping and functional characterization of Arabidopsis phototropin 1. *Mol Plant* 1:178–194.
30. Thingholm TE, Larsen MR (2009) The use of titanium dioxide micro-columns to selectively isolate phosphopeptides from proteolytic digests. *Methods Mol Biol* 527: 57–66, xi.